Challenges in the Localization of a UHF Radio Pill in the Gastro-Intestinal Tract

Camille Aubry
Biomedical Engineering, Faculty of Medicine Nancy.
University of Lorraine
Nancy, France
camil.aubry@orange.fr

David V. Thiel
Griffith School of Engineering
Griffith University
Nathan, Qld Australia
d.thiel@griffith.edu.au

Hugo G. Espinosa
Griffith School of Engineering
Griffith University
Nathan, Qld Australia
h.espinosa@griffith.edu.au,

Esmaeil S. Nadimi
Maersk Mc-Kinney Institute, Faculty of Engineering
University of Southern Denmark
Odense, Denmark
esi@mmmi.sdu.dk

***Abstract*—Visual and chemical investigations in the gastro-intestinal tract using injected "pill" sized sensors are challenging. The throughput takes between 24 and 48 hours and a precise location accuracy to less than 5 cm is necessary for keyhole surgery. Model and computational experiments using a 433 MHz subsurface transmitter in a saline (conductivity = 0.2 S/m) tank show that location accuracy is compromised by non-conducting boundaries between internal organs connected by non-conducting interstitial tissue. The internal transmitter profile changes significantly by the presence of insulating boundaries modelled by non-conducting boundary in an otherwise uniform conducting medium. A worn sensor array in the front of the abdomen can define the location of a GI pill only if there is significant information about the internal organ configuration.**

Keywords—gastrointestinal tract; radio pill; UHF location

I. INTRODUCTION

The gastrointestinal (GI) tract in humans is long, delicate and difficult to investigate without major surgical intrusion. Optical fibre (endoscope) investigations can only cover small parts of the GI tract. While GI "pills" have shown promise for many years [1] in detecting such abnormalities as polyps and bleeding, the location of these abnormalities can only be approximated by the time delay between entry and identification. More recently, such investigations have been accompanied by a video camera [2], however the location of the image where abnormalities have been found during the 24-48 hour passage through the gut is highly variable and so presents a major challenge. In an ideal system the patient would wear a garment fitted through the 24-48 hours. The garment would be equipped with detection sensors to locate and record the radio signals.

Since capsule localization is directly based on the estimation of the distance between the capsule and a set of receivers placed outside the body, enhancing the estimation of this distance results in localization improvement. Various methods have been introduced for distance estimation, such as magnetic field intensity [3, 4], time of arrival (TOA) [5] and the received signal strength indicator (RSSI) [6, 7]. The magnetic-based and the TOA-based solutions have received less attention than the RSSI-based solutions due to the fact that the first ones enlarge the capsule (since they need a permanent or a transient magnet) while the second ones require precise synchronization between the transmitter and the receiver, at the cost of extra synchronous clocks. The RSSI-based solutions, on the other hand, have been more attractive for many researchers due to their simplicity and low cost, even though they suffer from low precision and high dependency on the propagation medium properties. Localization of an endoscopic capsule for GI tract monitoring with an error margin up to 5 cm is acceptable [8].

II. EQUIPMENT AND SETTINGS

An identical pair of battery powered radio transmitters (433 MHz, +10 dBm) were used to detect the received signal strength (RSSI) between them. The unit consisted of a ground plane containing the circuit electronics (4 cm × 6 cm) and a quarter wave length whip antenna (17 cm) (Fig. 1).

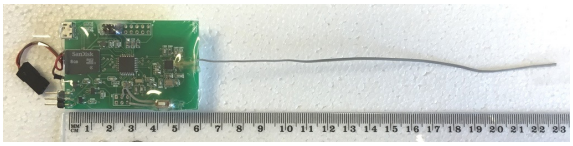

Fig. 2. 433 MHz radio transmitter beacon used to detect the received signal strength (RSSI). A second identical beacon was used as transmitter.

One unit was enclosed in a water proof plastic bag and placed inside a rectangular water-filled container (90 × 34 × 38 cm^3) (Fig. 2). The water temperature averaged 19°C throughout the measurements. The water was doped with NaCl to a conductivity of σ = 0.2 S/m. This conductivity corresponds to

the conductivity of internal organs of humans [9, 10]. At 433 MHz, the permittivity was $\varepsilon = 79\varepsilon_0$ F/m. The conductivity was measured using an LC81 conductivity meter from TPS Pty Ltd with appropriate temperature compensation.

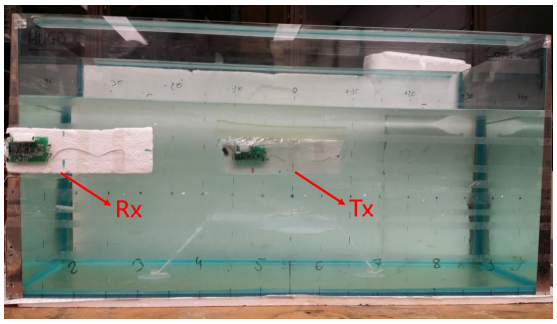

Fig. 2. Set up of the transmitter inside the rectangular tank filled with a saline water solution, and the receiver located outside the boundary of the tank.

The second transceiver was located at the front of the container and moved across the outer surface in steps of 5 cm. The RSSI was recorded for approximately 25 seconds at each point. Both radio beacons were oriented parallel to each other for maximum signal reception. While both beacons recorded the received signal strength, one recorded a higher level as the power of the transmitter differed slightly between the two beacons. The maximum, undistorted signal strength that could be recorded was -20 dBm and the minimum detectable level was -97 dBm. As the communications between the two beacons was via received packets, the possibility of received signal interference was very low and could not be determined experimentally.

While initial measurements were directed at gaining information about the unperturbed signal as a function of distance across the face of the container, thin walled PVC pipes were added inside the solution to imitate the effect of insulating boundaries between organs in the abdomen. A 40 cm length PVC pipe with dimensions (10 cm × 5 cm) used in various configurations was open at one end and filled with the same saline water as that surrounding the transmitter and with a different conductivity that corresponds to different internal organs, for example, the conductivity inside the small intestine.

III. Numerical Modelling

A two dimensional forward modelling impedance method [11] was used to model the electric field signal strength on the surface of the water-filled container. This method requires the solution space to be discretized into 2-dimensions using rectangular cells bounded by impedance elements with properties dependent on the local electromagnetic properties of the medium and the cell size. The model consisted of a rectangular grid defined by 90 cm length and 38 cm depth with 1 cm cell resolution. The transmitter was located inside the water ($\sigma = 0.2$ S/m, $\varepsilon_r = 79$) located 20 cm from the water/air boundary, and the receiver was located in the outside boundary of the water tank.

The current vectors inside the water tank were simulated for two different situations: with the transmitter located inside the water-filled container (Fig. 3a), and with the transmitter located inside a thin walled rectangular PVC pipe, and a parasitic adjacent rectangular pipe located 5 cm from the pipe's boundary (Fig. 3b). The currents are contained inside the pipe, which is resonating with two current loops. The shape is due to the rectangular discretization of the model. A second order resonance can be observed in the parasitic pipe with circular currents.

The electric field at the water/air boundary was determined as the product between the surface impedance and the magnetic field [11]. The magnetic field was computed through the solution of the linear system $[\mathbf{S}]_{N\times N}[\mathbf{H}]_{N\times 1} = [\mathbf{H}_0]_{N\times 1}$, where $\mathbf{H}$ is the vector of unknown magnetic field elements, $\mathbf{H}_0$ is the known source field vector, $\mathbf{S}$ is a square, side-banded tri-diagonal sparse matrix and N is the number of impedance elements in the solution space. Since the forward modelling in is in two dimensions, both the transmitter inside the water tank and the receiver outside the tank were aligned so the horizontal cross section was simulated.

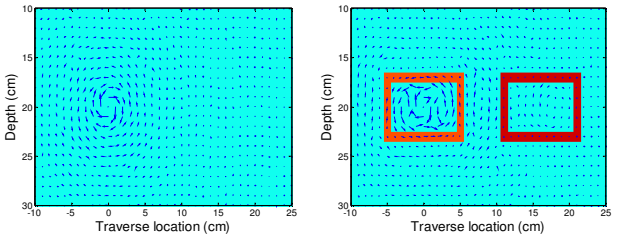

(a) (b)

Fig. 3. Current vectors of (a) transmitter inside the water-filled container, and (b) transmitter located inside a rectangular PVC pipe with a parasitic adjacent pipe at 5 cm.

The electric field strength (in dBm) was calculated for the following cases: Transmitter (Tx) inside the water-filled tank, transmitter inside a rectangular PVC pipe, and transmitter inside a rectangular pipe with a parasitic adjacent pipe. The separation distance between the two pipes was varied from zero to 30 cm. Figure 4 shows the electric field strength in dBm for all cases. The separation between the pipes is 15 cm and 25 cm.

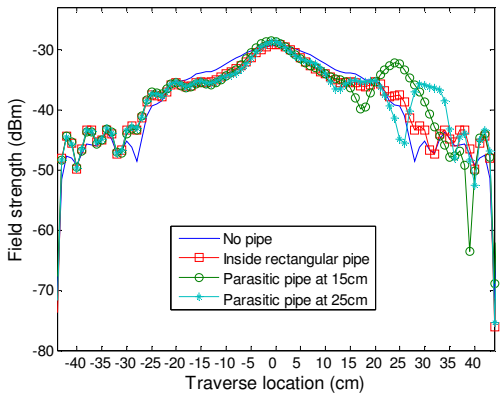

Fig. 4. Numerical modelling of the electric field profiles (dBm) across the surface of the tank, with the transmitter inside a rectangular pipe and a parasitic adjacent pipe located at different distances from the transmitter.

It can be observed from Fig. 4 that the presence of the pipe around the beacon significantly reduces the half-power beam width. The presence of the second pipe on the right side creates a second side peak which moves as the separation distance between the two pipes increases.

IV. Experimental Results

The experimental results for an immersed transmitter were plotted as a function of distance across the face of the container (Fig. 2). In Section III the electric field strength was calculated for different scenarios. Since the receiver records a signal every second, the results presented in the following sections *A* and *B* were determined using the mean value of the 25 seconds recorded at each point.

A. Transmitter inside a rectangular PVC pipe and the effect of adjacent parasitic pipes

In the first experiment (Fig. 5), the transmitter was immersed and located at the center of the water-filled tank, 19 cm from the boundary where the measurements were taken. The measurements were compared with those obtained with the transmitter located inside a rectangular PVC pipe and two adjacent parasitic pipes with a separation distance varying from 0 to 30 cm. Figure 5 shows the parasitic pipe at 15 cm and 25 cm from the source. The conductivity inside the pipe was the same as the conductivity in the main tank.

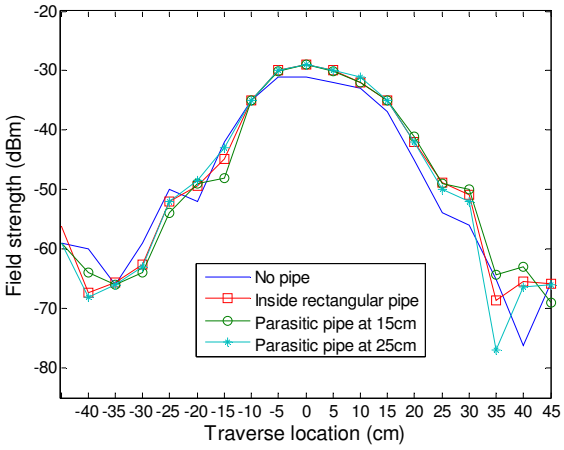

Fig. 5. Measurements of the electric field profiles (dBm) across the surface of the tank, with the transmitter located inside a rectangular pipe and a parasitic adjacent pipe located at different distances from the transmitter.

As in Fig. 4, it can be observed from Fig. 5 that the presence of the pipe around the beacon distorts the surface electric field due to the disruption of the current, and increases the field strength. However, the beam width does not reduce as occurred in the modelling. The presence of the adjacent second pipe also creates a lobe to the right side, but the separation between pipes does not affect the location of the parasitic lobe. The distortions above 30 cm and below -30 cm are reflections due to the finite size of the water-filled tank.

B. The effect of pipes with different shapes and conductivities

In a more realistic situation the radio pill would travel through a circular-shaped intestine with a different conductivity between the inside and the outside. Therefore, two more experiments were conducted. In the first one (Fig. 6), the transmitter was located inside a circular PVC pipe with an adjacent parasitic circular pipe located 10 cm next to it. The measurements were compared with those obtained using the same arrangement but rectangular pipes instead.

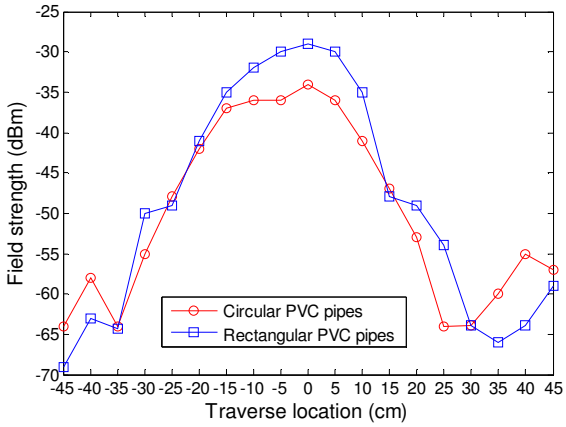

Fig. 6. Measurements of the electric field profiles (dBm) across the surface of the tank with the transmitter located inside a rectangular pipe and a circular pipe, both with an adjacent parasitic pipe with the same shape.

It can be observed from Fig. 6 that the field strength decreases in the circular pipe. Additionally, the feature of the adjacent parasitic pipe is more significant when a rectangular pipe is used.

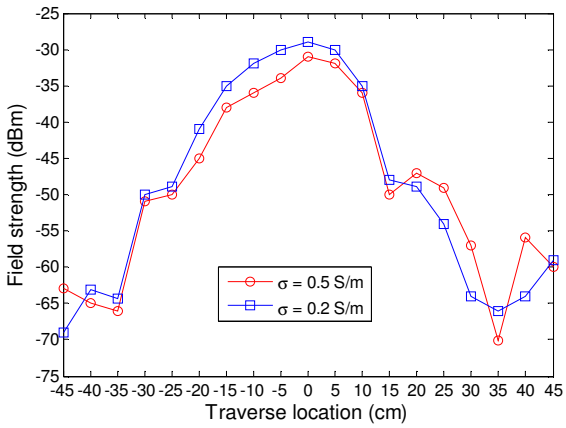

Fig. 7. Measurements of the electric field profiles (dBm) across the surface of the tank with the transmitter located inside a rectangular pipe and an adjacent pipe, both with conductivities $\sigma = 0.5$ S/m and $\sigma = 0.2$ S/m.

In the second experiment (Fig. 7), the transmitter was located inside a rectangular pipe with a conductivity of $\sigma = 0.5$ S/m that corresponds to the conductivity of the small intestine [9, 10]. An adjacent parasitic rectangular pipe with the same conductivity was located 10 cm next to it.

The results were compared with those obtained for a conductivity σ = 0.2 S/m inside both the source and the adjacent pipes.

It can be observed from Fig. 7 that the field strength decreases when the conductivity is different between the inside and the main tank. In addition, the location of the parasitic adjacent pipe when σ = 0.5 S/m can be clearly determined.

C. *Statistical analysis for significant differences between electric field profiles*

To study the dissimilarity between the field strength in circular and rectangular PVC pipes with σ = 0.2 S/m and σ = 0.5 S/m, the coupling measure metric using discrete Frechet distance was estimated. The distance is a measure of the minimum length of a line sufficient to join a point traveling forward along the curves while the rate of travel for either point may not necessarily be uniform [12]. In this study the raw data was used, so every data point was considered for the statistical analysis.

Figure 8a shows the three curves to be analyzed: transmitter inside a rectangular pipe with σ = 0.2 S/m, inside a rectangular pipe with σ = 0.5 S/m and inside a circular pipe with σ = 0.2 S/m. The conductivity in the main tank was σ = 0.2 S/m.

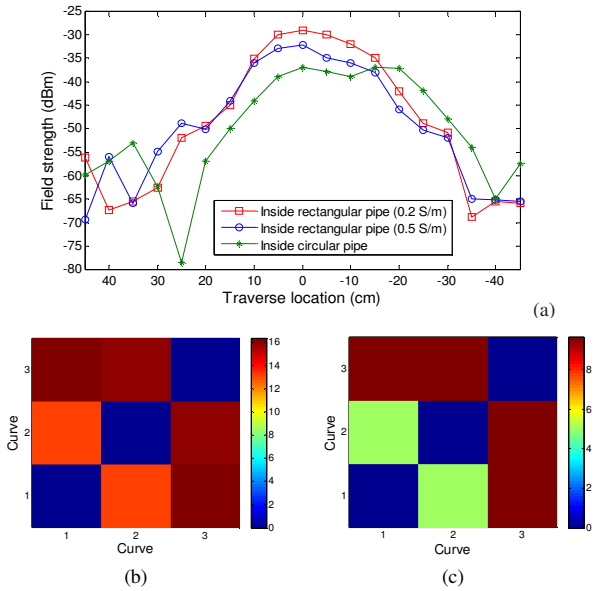

Fig.8. (a) Field strength for a transmitter inside circular and rectangular pipes with σ = 0.2 S/m and σ = 0.5 S/m, (b) Curve analysis using Frechet distance and (c) curve analysis using root mean squared distance (RMSD).

The entities of the image matrix in Fig. 8 correspond to the Frechet distance (Fig. 8b) and root mean squared distance (RMSD) (Fig. 8c) between the field strengths of the three experimental configurations. It can be observed that the largest Frechet and RMS distances are between curves 1 and 3 associated with the field strength in rectangular (σ = 0.2 S/m) and circular pipes, respectively. The results show that the shape of the pipe has a higher impact on the field strength compared to the variation of conductivity.

V. CONCLUSIONS

A preliminary investigation in the location of a radio pill in the gastro-intestinal tract was conducted. Both numerical and measurements experiments were performed on a 433 MHz radio transmitter immersed in a water tank filled with a saline solution. An impedance method-based forward modelling algorithm with rectangular discretization was used for the numerical experiments, in which the electric field strength increased when the transmitter was located inside a thin walled rectangular pipe. The location of adjacent parasitic pipes was clearly identified. Measurements showed an increase in the field strength with immersed pipes. However, the location of second side peaks from adjacent parasitic pipes did not change with the increase in the separation between the two pipes. A different conductivity inside the pipes to that from the main tank showed a better feature in the parasitic pipe. The field profile was affected by the insulating boundaries. The Frechet and RMS distances showed significant differences between the rectangular and circular pipes.

REFERENCES

[1] A.M. Connell, J. McCall, J.J. Misiewicz, and E.R. Rowlands, "Observations on the clinical use of radio pills," British Medical Journal, pp. 771-774, Sept. 1963.

[2] D. Panescu, "An imaging pill for gastrointestinal endoscopy," IEEE Engineering in Medicine and Biology magazine, vol. 24, no. 4, pp. 12-14, Jul. 2005.

[3] C. Hu, M.Q.H. Meng, and M. Mandal, "Efficient magnetic localization and orientation technique for capsule endoscopy," International Journal of Information Acquisition, vol. 2, no. 1, pp. 23-36, 2005.

[4] M. Salerno, G. Ciuti, G. Lucarini, R. Rizzo, P. Valdastri, A. Menciassi, A. Landi, and P. Dario, "A discrete-time localization method for capsule endoscopy based on on-board magnetic sensing," Measurement Science and Technology, vol. 23, no. 1, pp. 1-10, 2012.

[5] K. Pahlavan, Y. Ye, R. Fu, and U. Khan, "Challenges in channel measurement and modeling for RF localization inside the human body," International Journal of Embedded and Real-Time Communication Systems, vol. 3, no. 3, 18-37, 2012.

[6] D. Fischer, R. Shreiber, G. Meron, M. Frisch, H. Jacob, A. Glukhovsky, and A. Engel, "Localization of the wireless capsule endoscope in its passage through the GI tract," Gastrointestinal Endoscopy, vol. 53, no. 5, 2001.

[7] D. Fischer, R. Shreiber, D. Levi, and R. Eliakim, "Capsule endoscopy: The localization system," Gastrointestinal Endoscopy Clin., North Amer., vol. 14, pp. 25-31, 2004.

[8] M.H. Ramezani, V. Blanes-Vidal, and E.S. Nadimi, "An adaptive path loss channel model for wave propagation in multilayer transmission medium," Prog. in Electromagnetics Research, vol. 150, pp.1-12, 2015.

[9] J.M. Osepchuk, "Biological effects of electromagnetic radiation," IEEE Press, 1983.

[10] E.S. Nadimi, V. Blanes-Vidal, J.L.F. Harslung, M.H. Ramezani, J. Kjeldsen, P.M. Johnsen, D.V. Thiel, and V. Tarokh, "In vivo and in situ measurement and modelling of intra-body effective completex permittivity," IET Health Care Technology Letters, (in press), 2015.

[11] H.G. Espinosa, and D.V. Thiel, "Efficient forward modelling using the self-consistent impedance method for electromagnetic surface impedance," Exploration Geophysics, vol. 45, no. 3, pp. 201-207, Jul. 2014.

[12] A. Efrat, L.J. Guibas, S. Har-Peled, J.S.B. Mitchell, and T.M. Murali, "New similarity measures between polylines with applications to morphing and polygon sweeping," Discrete and Computational Geometry, vol. 28, no. 4, pp. 535-569, 2002.